System Performance Measurements for an All-Optical Header Processor Using 100-Gb/s Packets

K. H. Ahn, *Member, IEEE,* J. W. Lou, *Student Member, IEEE,* Y. Liang, O. Boyraz, *Student Member, IEEE,* T. J. Xia, *Member, IEEE,* Y.-H. Kao, *Member, IEEE,* and M. N. Islam, *Senior Member, IEEE*

***Abstract*— We experimentally measure the eye diagram of an all-optical header processor using a crosscorrelator to achieve picosecond resolution. By varying 100-Gb/s header packets, we measure an eye diagram with a Q-value of 7.1 at 12-pJ packet pulse energy for the all-optical header processor consisting of all-optical logic gates and synchronized fiber lasers. From the Q-value, we also statistically calculate the potential bit-error-rate performance of 7.0×10^{-13}. By measuring the change in Q-values as a function of input power, we find that input power fluctuations degrade the performance of the header processor by reducing the switching contrast of the logic gates in the header processor.**

***Index Terms*— Communication system performance, optical fiber communication, optical logic gates, optical signal processing, packet switching.**

AS ULTRAFAST, all-optical, telecommunication devices start to push the single channel speeds beyond 100 Gb/s, measurement techniques must also be devised to test the performance of these all-optical devices. Currently, the method to measure the performance of a telecommunication device is to use a bit-error-rate (BER) tester, which sends a long bit pattern to the test device and counts the number of errors that occur through the device. However, these BER testers are currently limited to about 15 Gb/s. Therefore, to overcome this limitation, we use a method based on a sampling technique [1], [2] using a crosscorrelator and reference. This allows the measurement of eye diagrams with picosecond resolutions. However, the speed of the technique is limited to the sampling speed. We apply this technique to an all-optical header processor consisting of two synchronized lasers [3], 100-Gb/s word encoders, and two logic gates in the form of nonlinear optical loop mirrors [4] (NOLM). The eye diagram has a Q-value of 7.1 at 12-pJ switching energy for the header processor. We believe that this technique has possible applications as a statistical monitor of potential system performance in high-speed optical networks. Although it can not be used to detect and/or correct specific errors in data packets, the technique gives a statistical Q-value from which a bit-error rate (BER) can be inferred.

Manuscript received September 2, 1998. This work is supported by the Defense Advanced Research Projects Agency, by the U.S. Department of Defense, and by the National Science Foundation.

The authors are with the Department of Electrical Engineering and Computer Science, The University of Michigan, Ann Arbor, MI 48109 USA.

Publisher Item Identifier S 1041-1135(99)00353-5.

Fig. 1 shows the detailed experimental setup. The sources for the header processor are the master laser, representing a transmitter and the slave laser, acting as the local laser. They are synchronized using an acoustooptic modulator (AOM)/grating pair [3]. Both lasers produce 2-ps pulses at 1535 nm with a repetition rate of 21.6 MHz. A 2.3-nm bandpass filter spectrally shapes the slave laser pulse used as the local address bit, making the pulse closer to transform-limited. The output from the master laser passes through the encoder consisting of two 1×4 couplers, to produce the packet pattern "0 001 011 100" with 10-ps bit-to-bit separations. Similarly, the output from the slave laser passes through the clock consisting of two 1×3 couplers to produce the 3-bit pattern "111." The inverter determines whether the incoming packet address is all "1's," corresponding to the special case for an empty packet, and the XOR gate determines if the addresses match. In the case when the packet is empty, the output of the first gate is "000." Likewise, when the addresses match, the output of the second gate is "000." We use a threshold detector to distinguish these two cases from the not-empty and unmatched cases which have at least one "1" in the output. The cascaded operation demonstrates multiple logic operations allowing for more complicated logic operations [4]. Crosscorrelator 2 is used to control timing drifts caused by thermal fluctuations.

The output of the header processor is split and sent to the diagnostics for performance analysis. By adjusting the relative timing between the master laser encoder and the slave laser encoder with a variable delay stage, we can obtain any one of eight possible 3-bit patterns. Crosscorrelator 1 is slightly modified by using the fast response ($\sim$10 ns rise and decay time, packet separation of $\sim$47 ns) of the photomultiplier tube (PMT) to remove any of the averaging effects. By using a digital scope to take single-shot scans of the signal from the PMT, a single-pulse response is taken per scan. We take a large number of scans while varying the timing between the reference pulse and the output of the header processor. Then, by overlaying the scans, we can map out the eye diagram with picosecond resolution for all the possible patterns.

The eye diagram for the header processor is shown in Fig. 2. The eye diagram is for return-to-zero, hyperbolic secant pulses, and it is an overlay of all possible outputs from the header processor. The input header is equally varied between all of the eight possible 3-bit combinations. The local address is "010"

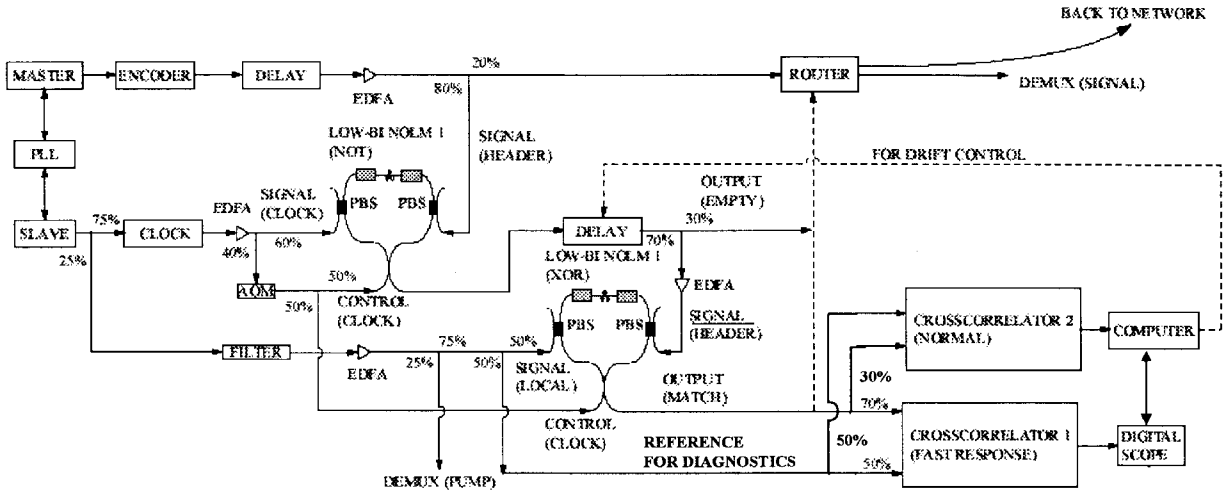

Fig. 1. Experimental setup. The master laser passes through the encoder producing "0001011100," and the Slave laser passes through clock producing "111." The output of the header processor, consisting of two NOLM's, is sent to crosscorrelator 1 for measuring the eye diagram. Crosscorrelator 2 is used for environmental drift control. PLL: Phase-locked loop. NOLM: Nonlinear optical loop mirror. AOM: Acoustooptic modulator. EDFA: Erbium-doped fiber amplifier. PBS: Polarization beam splitter.

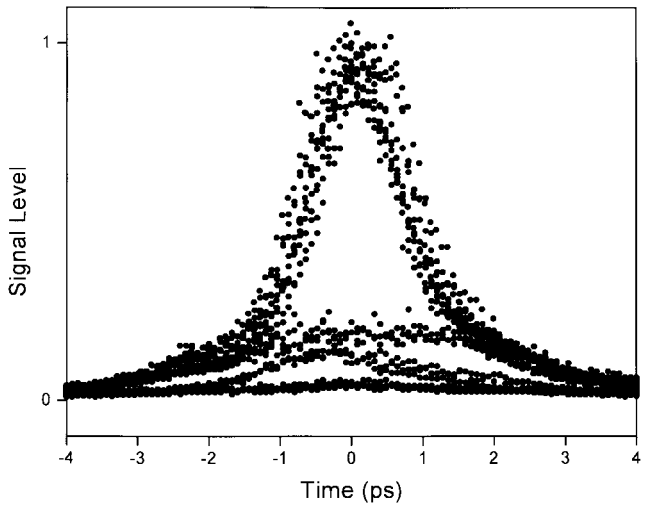

Fig. 2. Eye diagram of header processor. This is the trace of the eye diagrams taken with the setup of Fig. 1 where the trace is taken by moving an optical delay stage in cross-correlator 1. It is an overlay of all the different possible combinations of the 3-bit incoming header and the two possible values of "0" or "1" for the local bit.

and thus, the local address bit may be a "1" or "0" depending on which bit is scanned. Because the NOLM has a finite polarization extinction ratio, there is pump leakage present. Consequently, in the XOR ($\wedge$) gate, the "0" level is different for the case without any pump pulses (i.e., $0 \wedge 0 = 0$) and for the case with two-pump pulses (i.e. $1 \wedge 1 = 0+$ leakage). This leads to a spread of the "0" level in the eye diagram. However, there is no such spread for the "1" level because the nonlinear transmission from the NOLM dominates any pump leakage.

By fixing the reference pulse at the center of the bit period, we can measure the Q parameter at the center of the eye opening from which we can statistically calculate the potential BER. The Q parameter is defined by $Q = (I_1 - I_0)/(\sigma_1 + \sigma_0)$ with I_1 and I_0 being the sampled means of the "on" and "off," respectively and with σ_1 and σ_0 being the sampled standard deviations of the "on" and "off," respectively [5]. The measured Q-value is an optical Q where we have neglected the relatively small electronic noise in the PMT. The statistical BER is given by BER $= 0.5 \times \text{erfc}\ (Q/\sqrt{2})$ where the erfc is the complementary error function. Note that by sampling in the middle of the eye, we are measuring the instantaneous response of the header processor output cross-correlated with a reference pulse. The resolution of the sample is determined by the pulsewidth of the reference pulse. Thus, the crosscorrelation technique takes only one sample point in the bit period but actually integrates the overlapped energy between the signal and the reference. For each 3-bit pattern, 150 data points are taken. Because there are eight different possible 3-bit patterns, the total number of data points is 1200. In addition, because the local bit can be "0" or "1," there are 1200 data points for the "1" level and the "0" level. With these points, we find a Q-value of 7.1, which corresponds to a BER of 7.0×10^{-13}.

Because this is a statistical method, we must look at the associated confidence interval to calculate possible errors in the measurement. The confidence interval is an interval of values that contains the true value of a parameter with a given confidence level. For a given system, the confidence interval for the mean [6] is given by

$$P\left[I_n - t_{n-1,1-\alpha/2}\,\frac{\sigma_n}{\sqrt{n}} < I_n + t_{n-1,1-\alpha/2}\,\frac{\alpha_n}{\sqrt{n}}\right] = 1 - \alpha \tag{1}$$

and the confidence interval for the variance is given by

$$P\left[\frac{(n-1)\sigma_n^2}{\chi^2_{n-1,1-\alpha/2}} < \sigma^2 < \frac{(n-1)\sigma_n^2}{\chi^2_{n-1,\alpha/2}}\right] = 1 - \alpha \tag{2}$$

where I_n is the sampled mean, μ is the (unknown) true mean, σ_n is the sampled standard deviation, σ is the (unknown) true standard deviation, n is the number of sampled points, and $(1-\alpha) \times 100\%$ is the confidence interval level. The $t_{v,p}$ and the $\chi_{v,p}$ are the standard t-distribution and the chi-square distribution, respectively, with subscripts being appropriately

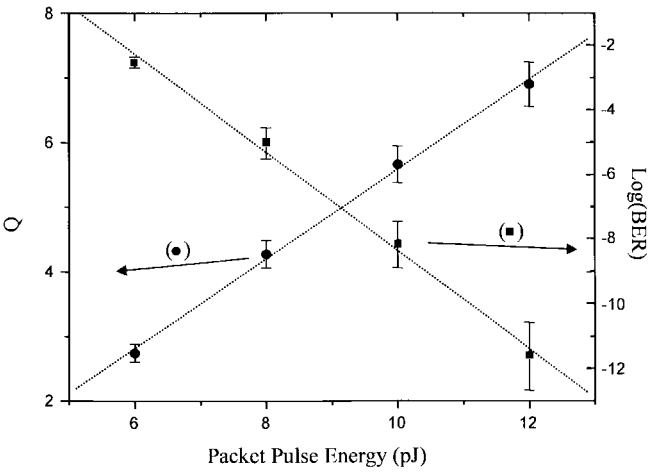

Fig. 3. (Left axis, circles)Q versus packet pulse energy. Looking at the center of the eye diagram for the "match" case and the "empty" case, we measure the Q-value while changing the pulse energy of the incoming packet. Calculated BER (right axis, squares) versus Packet Pulse Energy. From the Q-values, we extrapolate the BER. Error bars are set for 95% confidence level for both axes.

substituted with the subscripts defined by the confidence intervals. By looking at the confidence interval and setting the confidence level to 95%, we can calculate the error range of the Q-value to be from 6.7–7.4 for the eye diagram of Fig. 2. This means a worst case BER of 8.8×10^{-12} and a best case BER of 4.8×10^{-14}. Note that this error range is inversely related to the number of sample points for a given confidence level.

To test the variation in parameters of this technique, we also look at the performance of the header processor as a function of input packet pulse energy. To study this, we measure the Q-value of the header processor while varying the pulse energies of the incoming packet. This is done for the two cases: the matched header ("101") and the empty packet header ("111"). For the matched header, the output of the header processor is "000," and for the empty packet header, the output is "010." We choose only two patterns to minimize the measurement time and to reduce the effects of long-term drift. For each pattern, we take 150 sample points at the center of the eye diagram so that there are 150 points for the "1" level and for the "0" level. Note that although we decrease our confidence level by taking fewer points, the Q is comparable to the 7.1 value mentioned above, which was derived from more sample points.

In Fig. 3, the circles show the results for the Q versus input packet pulse energy, and the squares show the extrapolated BER versus input packet pulse energy. The error bars on the data points are calculated with a 95% confidence interval level, and the range of the error bars is defined by the confidence interval. Because the ratio of error range over the measured value is nearly constant for a given confidence level, the error bars are larger for the higher Q-values (lower BER). We find that both the Q-values and the corresponding BER values degrade linearly with the input power. For example, we find that there is a 40% degradation of the switching contrast for the logic gates at input pulse energy of 7 pJ.

Although the results are reasonable, there are some limitations for the sampling technique. First, while the eye diagram is measured experimentally, because of the lack of long bit patterns, there is no information related to intersymbol interference (ISI). However, because the header processor would only look at packet headers at the packet rate and not at long streams of bits, the lack of ISI may not be so detrimental. Second, the BER values are calculated statistically from the eye diagram assuming a Gaussian noise distribution. Therefore, this may give an inaccurate value for the BER. However, the Gaussian assumption generally underestimates the performance because the major contribution of noise is from the amplifiers, which have an exponential noise distribution [7]. Finally, because the BER measurement is a statistical measurement, there is an error bar (confidence interval) associated with the value. This error bar is related to the number of data points (or bits) taken in the sample. For example, for the 1200 points of Fig. 2, the error of the Q-value is $\pm 5\%$, and for the 150 points of Fig. 3, the error of the Q-value is $\pm 13\%$. Consequently, the method can be improved in accuracy by using more points (or bits). In a real system, the data acquisition rate may be increased by demultiplexing the packet to a slower bit rate and then using a high-speed detector.

In conclusion, we demonstrate a measurement technique with picosecond resolution used to test the performance of an all-optical header processor. The header processor consists of two synchronized fiber lasers driving two all-optical logic gates and exhibits an eye diagram with a Q-value of 7.1 for 100-Gb/s header packets. We statistically calculate a BER value of 7.0×10^{-13} from the Q-value of the eye diagram. Assuming a 95% confidence level, the error on the Q-value is $\pm 5\%$ for 1200 data points. Also, we find that power fluctuations of the incoming packet headers linearly degrades the Q parameter of the header processor, primarily due to a degradation of the logic gate switching contrasts with the switching contrast down by 40% at 7 pJ. The development of measurement techniques for high-speed systems is an important and necessary step in constructing all-optical networks.

REFERENCES

[1] T. Kanada and D.L. Franzen, "Optical waveform measurement by optical sampling with a mode-locked laser diode," *Opt. Lett.*, vol. 11, no. 1, pp. 4–6, 1986.

[2] H. Takara, S. Kawanishi, and M. Saruwatari, "Optical signal eye diagram measurement with subpicosecond resolution using optical sampling," *Electron. Lett.*, vol. 32, no. 15, pp. 1399–1400, 1996.

[3] M. Jiang, K. H. Ahn, X.-D. Cao, P. Dasika, Y. Liang, M. N. Islam, A. F. Evans, R. M. Hawk, D. A. Nolan, and D. L. Weidman, "Synchronization of passively mode-locked Erbium-doped fiber lasers and its application to optical communication networks," *J. Lightwave Technol.*, vol. 15, pp. 2020–2028, Nov. 1997.

[4] K. H. Ahn, X. D. Cao, Y. Liang, B. C. Barnett, S. Chaikamnerd, and M. N. Islam, "Cascadability and functionality of all-optical low-birefringent nonlinear optical loop mirror: Experimental demonstration," *J. Opt. Soc. Amer. B*, vol. 14, no. 5, pp. 1228–1236, 1997.

[5] G. P. Agrawal, *Fiber-Optic Communication Systems*. New York: Wiley, 1992.

[6] R. M. Bethea, B. S. Duran, and T. L. Boullion, *Statistical Methods for Engineers and Scientists*. New York: Marcel Dekker, 1995.

[7] D. Marcuse, "Derivation of analytical expressions for the bit-error probability in lightwave systems with optical amplifiers," *J. Lightwave Technol.*, vol. 8, pp. 1816–1823, Dec. 1990.